JCZ: Zoologischer Anzeiger - A Journal of Comparative Zoology 300 (2022) 27–40

Contents lists available at ScienceDirect

Zoologischer Anzeiger

journal homepage: www.elsevier.com/locate/jcz

Comparative evaluation of coelomocytes in *Paracentrotus* sea urchins: Description of new cell types and insights on spherulocyte maturation and sea urchin physiology

Vinicius Queiroz [a,b,*], Vincenzo Arizza [b], Mirella Vazzana [b], Márcio R. Custódio [a]

[a] Departamento de Fisiologia, Instituto de Biociências, Universidade de São Paulo, São Paulo, Brazil
[b] Dipartimento Scienze e Tecnologie Biologiche Chimiche e Farmaceutiche (STEBICEF), Università degli Studi di Palermo, Palermo, Italy

ARTICLE INFO

Corresponding Editor: Carsten Lueter

Keywords:
Crystal cell
Cytology
Granular spherulocyte
Maturation process

ABSTRACT

Sea urchins are the best-known models in echinoderm immunology and only four coelomocytes – *i.e.* phagocytes, vibratile cells, and red and colorless spherulocytes – have traditionally been observed in these animals. However, recent studies have demonstrated that this number could be underestimated, which consequently may hinder a better understanding of sea urchin physiology. Here, we investigated the cells of one of the most known sea urchin genera in the world: the genus *Paracentrotus*. This genus comprises two species with distinct geographic distributions, thus providing an excellent scenario for comparative analyses. In this context, through an integrative approach consisting of living cells, cytological preparations, and scanning electron microscopy (SEM), we analyzed morphological, morphometric, and cytochemical characteristics of the coelomocytes of *Paracentrotus lividus* (Lamarck, 1816) and *Paracentrotus gaimardi* (Blainville, 1825). Seven different coelomic subpopulations were found in these species, including the traditional types and the granular spherulocyte, crystal cell, and progenitor cell. For all spherulocyte subpopulations, a set of morphologically similar cells were observed in both cytological and SEM preparations. Based on morphology, morphometry, and cytochemistry, we observed that these morphotypes could be organized in a sequence, which we interpreted as a maturation process. Then, we raise one hypothesis that explains how spherulocytes mature. Lastly, taking into account the all results achieved by this study, we discuss (1) how the morphological, morphometric, and cytochemical characteristics observed in *Paracentrotus* coelomocytes may be used to identify the coelomocytes of other sea urchins; (2) the physiological implications of our findings. Considering that *P. lividus* is one of the most studied sea urchins in the world, the new findings obtained here may shed new light on traditional aspects of sea urchin immunology (*e.g.* coelomocytes function), as well as stimulate research on new aspects of Echinoidea and even in Echinodermata immunology.

1. Introduction

Echinoids, commonly known as sea urchins, are widely used as models in several biological and biotechnological fields. These animals are valuable in basic research, such as developmental biology (McClay, 2011), genetics (Sodergren et al., 2006), or ecology (Precht and Precht, 2015). They are also used in applied studies, such as environmental monitoring (*e.g.* Alves et al., 2018; Vazzana et al., 2020), bioactive compound prospecting (Bragadeeswaran et al., 2013), and biomaterials research (Ferrario et al., 2020). Some species and genera are also quite important models for studies on human physiology (*e.g.* aging biology – Bodnar and Coffman, 2016), and immunology.

Much like vertebrates, the innate immune system in echinoids consists of humoral and cellular responses (Chiaramonte and Russo, 2015). Recent studies on basic cellular/molecular and systemic sea urchin immune responses (Arizza et al., 2007; Queiroz et al., 2021a) have pointed these responses as good indicators to evaluate the overall health status (Queiroz, 2020a) and effects of environmental stress (Pinsino and Matranga, 2015) in these animals. Although there is an increase in the number of studies analyzing echinoid humoral responses (*e.g.* Chiaramonte et al., 2020), works on cellular effectors (*i.e.* the coelomocytes) are far more numerous (Arizza et al., 2007; Alves et al., 2018;

* Corresponding author. Departamento de Fisiologia, Instituto de Biociências, Universidade de São Paulo, Rua do Matão, nº 321, Cidade Universitária, São Paulo, SP, 05508-090, Brazil.
E-mail addresses: vinicius_ufba@yahoo.com.br, vinicius.bio.ufba@gmail.com (V. Queiroz).

https://doi.org/10.1016/j.jcz.2022.06.008
Received 22 February 2022; Received in revised form 28 June 2022; Accepted 29 June 2022
Available online 6 July 2022

Chiaramonte et al., 2019). Functional and morphological studies on immune aspects of several echinoid species have been performed, including tropical, temperate, and polar organisms (e.g. Majeske et al., 2013; Gonzalez-Aravena et al., 2015; Queiroz, 2020a). In this context, the genus *Paracentrotus* Mortensen, 1903 stands out as one of the most well-studied sea urchin group.

Paracentrotus comprises two species, *i.e. Paracentrotus gaimardi* (Blainville, 1825) and *Paracentrotus lividus* (Lamarck, 1816) (Calderón et al., 2009), both well-known for their astonishing and intriguing color polymorphism (Boudoresque and Verlaque, 2013; Duarte et al., 2016). *Paracentrotus lividus* is a common Mediterranean species, whose geographic distribution ranges from Scotland and Ireland to Southern Morocco and the Canary Islands, including the Mediterranean (Boudoresque and Verlaque, 2013; Pantazis, 2009). By contrast, *P. gaimardi* is a little-known echinoid restricted to Africa (from the Gulf of Guinea to Angola) and Brazil (from Rio de Janeiro to Santa Catarina) (Mortensen, 1943; Calderón et al., 2010).

At the very least, the available data on the biological aspects of *Paracentrotus* are unbalanced. While *P. gaimardi* was investigated mostly due to its color polymorphism (Calderón et al., 2010; Lopes and Ventura, 2012; Duarte et al., 2016), *P. lividus* is one of the most well-known echinoids on the planet, with studies in all fields of knowledge. The conspicuous difference in the number of studies is not only due to its commercial significance (Pantazis, 2009) but also because *P. lividus* is used as a model in basic and applied research (*e.g.* Schillaci et al., 2014). This species is widely used as a model in physiology (Arizza et al., 2013), cellular and molecular biology (Cervello et al., 1994), as well as immunology (Arizza et al., 2007).

The immune mechanisms of *P. lividus* are relatively well studied, mainly regarding coelomocytes, which are the circulating cells in the coelomic fluid. The main cell populations are already described (Matranga et al., 2005), and their morphology was properly depicted in light and transmission electron microscopy (Deveci et al., 2015). Phagocytes in *P. lividus* are also responsible for the removal of foreign particles (Arizza et al., 20013), while red and colorless spherulocytes are connected to bacterial growth inhibition (Gerardi et al., 1990) and cytotoxicity (Arizza et al., 2007), respectively. Still, pathogen-associated molecular patterns (PAMPs), toxic metals, and nanoparticles can modulate coelomocyte activity (Pagliara and Stabili, 2012; Pinsino et al., 2015; Romero et al., 2016). Though much of the current knowledge on sea urchin coelomocytes is based on *P. lividus* (Smith et al., 2006; 2018), there is no information on the immune aspects of *P. gaimardi*, and even its coelomocyte types have not yet been described.

Even though most studies on sea urchins consider only four coelomic cell types (*i.e.* phagocytes, vibratile cells red, and colorless spherulocytes – Branco et al., 2013; Chiaramonte et al., 2019; Work et al., 2020), this number may be underestimated. For example, three different subpopulations of phagocytes (*i.e.* discoidal, polygonal, and small phagocytes) were described for *Strongylocentrotus droebachiensis* (Smith et al., 2006; 2010), while a new spherulocyte subpopulation, named granular spherulocyte, was found in *Eucidaris tribuloides*, *Arbacia lixula*, *Echinometra lucunter,* and *Lytechinus variegatus* (Queiroz and Custódio, 2015; Queiroz et al., 2021b). Though *E. lucunter* and *L. variegatus* are important models in echinoderm immunology (*e.g.* Faria and Silva, 2008; McCaughey and Bodnar, 2012; Branco et al., 2013), this new cell type is a recent discovery (Queiroz et al., 2021b).

In this context, this work aims to characterize the coelomic cells of *Paracentrotus* sea urchins from a comparative perspective. We used an integrative approach based on morphological and morphometric data to investigate the coelomocytes of *P. lividus* and the poorly known *P. gaimardi*. This genus comprises two species with distinct geographic distributions, thus providing an excellent scenario for comparative analyses. Data from light microscopy of living and stained cells, as well as scanning electron microscopy, were used to characterize the coelomocytes of these two echinoids, revealing new cell types for both species. Additionally, morphological and morphometric analyses of spherulocytes revealed a set of different but closely related morphotypes in all spherulocyte subpopulations, which can be understood as a putative maturation process. Based on our detailed characterization, we suggest the use of our data as a general guide to identifying sea urchin coelomocytes. Lastly, we take the opportunity to discuss the implications of our findings for sea urchin physiology.

2. Material and methods

2.1. Animals, bleeding procedure, and cell counting

Specimens of *P. gaimardi* ($n = 6$) were collected by free diving at Praia Grande, São Sebastião, São Paulo, Brazil (23°49′24″ S, 45°25′01″ W), while specimens of *P. lividus* ($n = 6$) were collected in the Gulf of Palermo, Palermo, Sicily, Italy (38°07.00′ N; 13°30.00′ E). For both species, coelomic fluid was sampled with a syringe preloaded with 0.5 ml isosmotic anticoagulant solution (20 mM ethylenediaminetetraacetic acid (EDTA), sodium chloride 460 mM, sodium sulfate 7 mM, potassium chloride 10 mM, 4-(2-hydroxyethyl)-1-piperazineethanesulfonic acid (HEPES) 10 mM, pH 8.2 – Dunham and Weissman, 1986). A 22 gauge needle (30 × 0.7 mm) was inserted into the coelomic cavity through the peristomal membrane and the same volume of coelomic fluid (0.5 ml) was withdrawn from each sea urchin. Total cell counts were made using a Neubauer chamber just after coelomic fluid sampling, and the results were adjusted to compensate for initial dilution. For differential cell counts, 1×10^6 cells/ml, and the proportion of main cell types were recorded under a light microscope. Considering that accurate cell counts need a relatively long time to be performed, and that such a long period can alter the shape and number of cells in the sample (Queiroz et al., 2022), colorless and granular spherulocytes were considered together in differential cell counts. We have adopted this protocol to avoid underestimated values for both spherulocytes in cell counts. Cell viability was determined by Trypan Blue assay (0.4%), according to Freshney (1987).

2.2. Morphological and morphometric analysis

Live cells in suspension were observed just after sampling, as described in Queiroz and Custódio (2015) and 25 cells of each type were measured, except for the rare crystal and progenitor cells, in which only five cells were measured. For cytological analyses, live cells were deposited on a slide using a cytocentrifuge (FANEN 248 simultaneous fluid removal cytocentrifuge, 6×10^4 cells per spot, 80×*g*/5 min), fixed for 45 min in formaldehyde sublimate, and stained with toluidine blue (TB) or Mallory's trichrome (MT) following standard protocols (Martoja and Martoja, 1967; Behmer et al., 1976). For scanning electron microscopy (SEM), live cells were deposited on round coverslips using the cytocentrifuge and fixed with formaldehyde sublimate. Afterward, the coverslips were washed once in Milli-Q water for 40 min, air-dried, and stored at room temperature in a closed container with silica gel. The coverslips were then sputter-coated with a 40–60 nm thick layer of gold and photographed in a Sigma VP (Zeiss) scanning electron microscope. For morphological descriptions, we employed the terms *flat* and *spread* with different practical meanings. *Flat/flatten* are used herein for cells in which the cytoplasm outline (*e.g.* phagocytes) is distinguishable, while *spread* is used for cells in which the cytoplasm is too thin to allow for the detection of the cell-substrate boundary (*e.g.* vibratile cells). The term *spherule* is also used herein to refer to the vacuole-like structures inside the spherulocytes.

Morphometry of the coelomocytes was based on digital images and carried out using ImageJ software (Schneider et al., 2012). Diameters of the cytoplasm and nucleus of 25 live cells were measured, and for live spherulocytes, the diameter of 30 cytoplasmic spherules (3 per cell) was also measured. For stained coelomocytes, diameters of cytoplasm and nucleus of 30 cells were measured. In the spherulocytes, we observed that each subpopulation (*i.e.* red, colorless, and granular spherulocytes) could be grouped in three different morphotypes, named M1, M2, and

M3. As we observed variation in M2, we divided it into M2A and M2B. These morphotypes were defined based on cytoplasm morphology and the gross size of the spherules, as previously observed in *Eucidaris tribuloides* (Queiroz and Custódio, 2015). As such, M1 indicates cells in the initial phase, M2 groups those within the continuous of intermediary morphologies, and M3 those at the end of the process. Subsequently, cytoplasm, nucleus, and spherule diameters were measured to confirm our assumption that those variations formed distinct groups. Thus, measurements of the nucleus and cytoplasm of 30 cells belonging to each morphotype ($n = 90$ cells for spherulocyte subpopulation; 270 cells/species) were performed. The nucleus/cytoplasm (N/C) ratio was also calculated by dividing the nucleus diameter by the cell length (cytoplasm + nucleus) of the same cell. For morphometric purposes, the M2A and M2B of all spherulocytes were considered together. Specifically, for stained red spherulocytes, the diameter of 45 spherules (3 per cell) per morphotype was measured ($n = 45$ cells per morphotype; 135 cells/species). Whenever the cytoplasm, nucleus, or spherules were not circular in outline, the Ferret diameter was considered.

2.3. Statistical analyses

Total and differential cell counts and measurements are presented as mean ± standard deviation, or mean ± standard deviation followed by a minimum–maximum value. Student's unpaired t-test was performed to analyze the differences between species. A two-way analysis of variance (two-way ANOVA) was used to analyze spherule diameter in live spherulocytes, using species and cell type as factors. We also used the two-way ANOVA to compare nucleus diameter, cytoplasm diameter, and nucleus/cytoplasm ratio among the different morphotypes of stained red, colorless and, granular spherulocytes, using species and morphotype as factors. Spherule diameters of stained red spherulocytes were compared using two-way ANOVA, using species and morphotypes as factors. Tukey multiple comparison *post hoc* tests were applied to Two-way ANOVA when necessary to understand the source of significance. To analyze the relation between spherule size and the stage of maturation, the spherule diameter of red spherulocytes was tested against the nucleus diameter of the same cell using a Pearson correlation. Differences in Student's unpaired t-tests and two-way ANOVA were considered significant if $p < 0.05$. All statistic analyses were performed in Prism 7 (Graphpad).

3. Results

Five cell types were found in both species: phagocytes, vibratile cells, red, colorless, and granular spherulocytes (Figs. 1 and 2). Crystal cells are small cells bearing a crystal-like structure in the cytoplasm, found only in *P. gaimardi*. Meanwhile, progenitor cells, coelomocytes with a disproportionally large nucleus, were found only in *P. lividus*. For all spherulocytes, a set of morphologically, morphometrically, and cytochemically similar cells were observed, and these morphotypes were named M1, M2 (A and B), and M3 (Figs. 3 and 4). Spherulocytes at M1 have a large nucleus and a homogeneous or lacy cytoplasm. In the M2 cells, the nucleus becomes smaller and more condensed and the spherules more evident. In cells belonging to M3, the nucleus had the smallest diameter among the morphotypes, as well as a cytoplasm filled with large spherules. Detailed analyses using SEM confirmed the pattern observed in cytochemical preparations (Fig. 4).

3.1. Total and differential cell counts

The total cell count in the coelomic fluid was similar for both species (Table 1). Except for the red spherulocyte, there was no significant difference in cell percentage between these sea urchins. Phagocytes were the most frequent subpopulation in both echinoids, but the frequency of the other populations differed (Table 1). For *P. gaimardi*, red spherulocytes were more frequent than colorless/granular and vibratile cells. By contrast, vibratile cells were the second most frequent type in *P. lividus*, followed by colorless/granular and red spherulocytes. Crystal cells from *P. gaimardi* and progenitor cells from *P. lividus* were rare, accounting for less than 1%. The trypan blue assay showed that cell viability was higher than 95% in all specimens.

3.2. Morphology and morphometry of living and stained mature coelomocytes

Live phagocytes were the largest cells (Table 2), usually with many filiform or bladder-like cytoplasmic expansions (Fig. 1A and M). Stained phagocytes were large round to oval flatten cells, with large central to subcentral nucleus (Table 2), and irregularly vacuolated cytoplasm (Fig. 1G and S). Vibratile cells were round and translucent when alive, with a conspicuous flagellum (Fig. 1B and N). In cytospin preparations, they are round, spread cells, filled with spherules containing proteoglycans, as indicated by the β-metachromasia (purple color) in TB preparations (Fig. 1H and T). We also observed two uncommon cell types: the crystal cell in *P. gaimardi* and the progenitor cell in *P. lividus*. Live crystal cells were small (Table 2), with a prominent translucent green crystal-like structure inside its cytoplasm (Fig. 1C). In cytological preparations, this spread cell showed no specific affinity to TB (Fig. 1I) or MT, but the intracellular crystals became darker with both stains. Although no nucleus could be detected in the crystal cell of *P. gaimardi*, this structure was found in crystal cells of other echinoderms, as depicted for *Apostichopus japonicus* and *Cucumaria japonica* through TEM and SEM analyses (Eliseikina and Magarlamov, 2002; Xing et al., 2008). Since few crystal cells were observed here, further studies are necessary to elucidate the basic morphophysiological aspects of this coelomocyte. Live progenitor cells exhibit a round to oval shape, with a relatively large nucleus (Table 2 and Fig. 1O) and the exact morphology can be seen in cytological preparations (Fig. 1U). The N/C ratio of this cell (0.77 ± 0.07) is very high in comparison with other cell types.

Live red and granular spherulocytes were usually round, with roundish uniform-sized spherules (Fig. 1D, F, P, and R), while the colorless showed an elongated profile, with spherules of various sizes and shapes (Fig. 1E and Q). In red spherulocytes, the spherules contained echinochrome, as indicated by the red color, and hyaline substances in granular and colorless spherulocytes (Fig. 1D–F and P-R). In addition to cell morphology, measurements of the spherules were also useful to identify each spherulocyte subpopulation (Fig. 5 and Table 3). Spherules in the colorless spherulocyte were significantly larger than those in red and granular ones, while comparisons between red and granular spherulocytes showed no differences (Table 3 and Fig. 5), and this pattern was evident in both species. Spherule diameter was not correlated with species ($F = 0.13$; $p = 0.7210$), but was associated with cell type ($F = 155.95$; $p < 0.0001$) and with the interaction between species and cell type ($F = 3.09$; $p = 0.0479$).

In cytochemical preparations, typical mature red spherulocytes (*e.g.* Fig. 1J and V) were very difficult to find, mainly in *P. lividus*. Red spherulocytes appeared as very flattened cells, sometimes tending to spread, with homogeneous round spherules which stain brownish in MT preparations (Fig. 1J and V *inset*) and dark blue in TB (Fig. 1V). However, mainly in *P. lividus*, the most common morphology of mature red spherulocytes in cytochemical preparations is an almost spread cell with round homogeneous empty vacuoles (Fig. 3D and P). Colorless spherulocytes showed large round to elongated spherules (Table 2), light blue with MT (Fig. 1K and W), and dark blue in TB slides. Granular spherulocytes showed small round homogeneous spherules (Table 2), similar in size to that of red spherulocytes. The granular spherulocyte stain reddish/pinkish with MT (Fig. 1L and X), but does not stain with TB, showing a grayish-blue color (Fig. 1X *Inset*).

3.3. Morphology of mature coelomocytes in SEM preparations

Phagocytes showed a quite flat and vacuolated cytoplasm, with

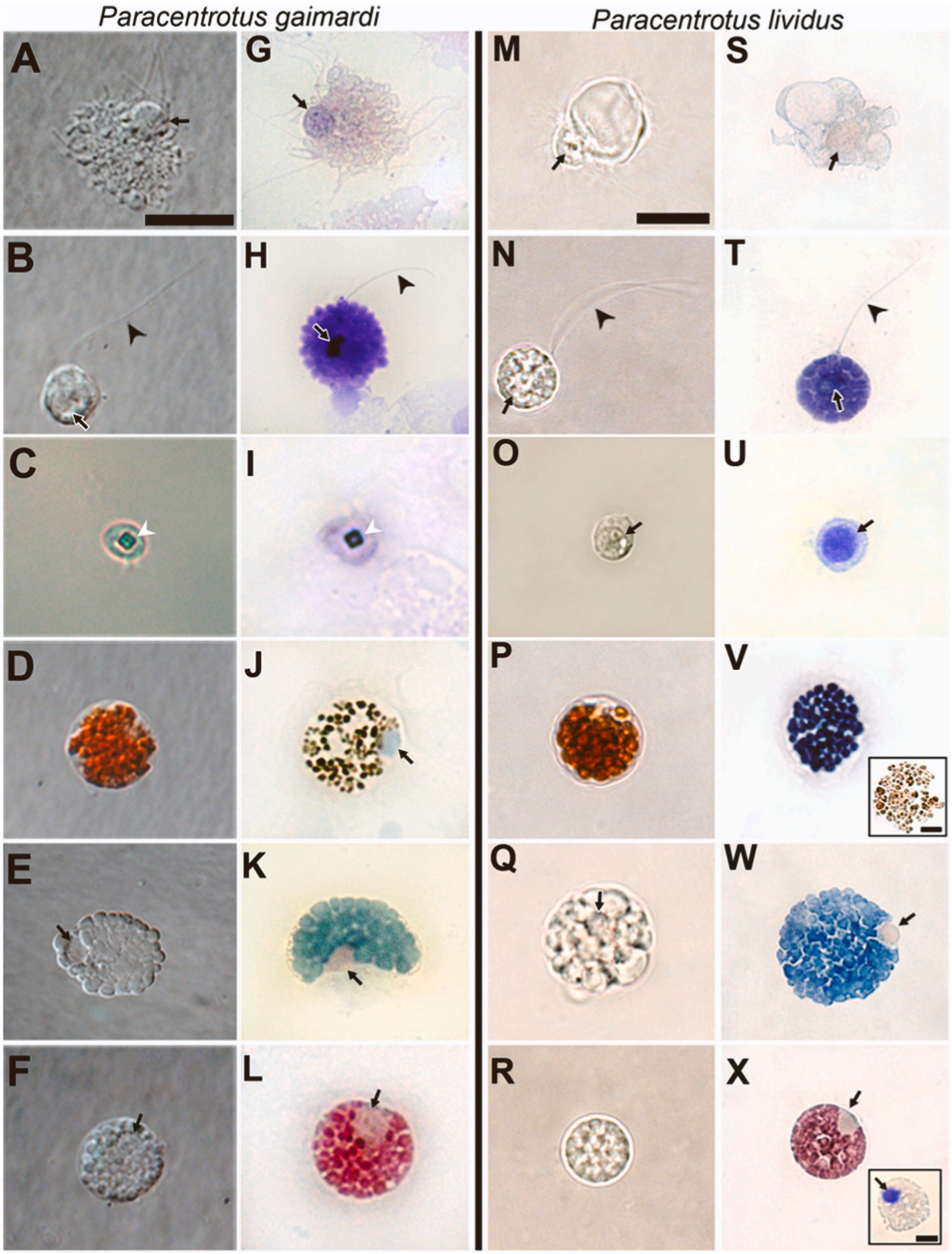

Fig. 1. Live and stained mature coelomocytes in *Paracentrotus* sea urchins. A-L – coelomocytes of *P. gaimardi*; M-X – coelomocytes of *P. lividus*. A, G, M, and S – Phagocytes; B, H, N, and T – Vibratile cell; C and I – Crystal cell; O and U – Progenitor cell; D, J, P, and V – Red spherulocyte; E, K, Q, and W – Colorless spherulocyte; F, L, R, and X – Granular spherulocyte. Columns A-F and M-R – Live cells; Columns G-L and S-X – Stained cells; A-B and D-F – Differential interference contrast; C and M-R – Light microscopy; G, J-L, S, V *inset*, W and X – Mallory's trichrome; H–I, T-V, and X *Inset* – Toluidine blue. Black arrowhead = Flagellum; white arrowhead = crystalloid; Arrow = nucleus. Scale: A-X = 10 μm; Insets = 5 μm. (For interpretation of the references to colour in this figure legend, the reader is referred to the Web version of this article.)

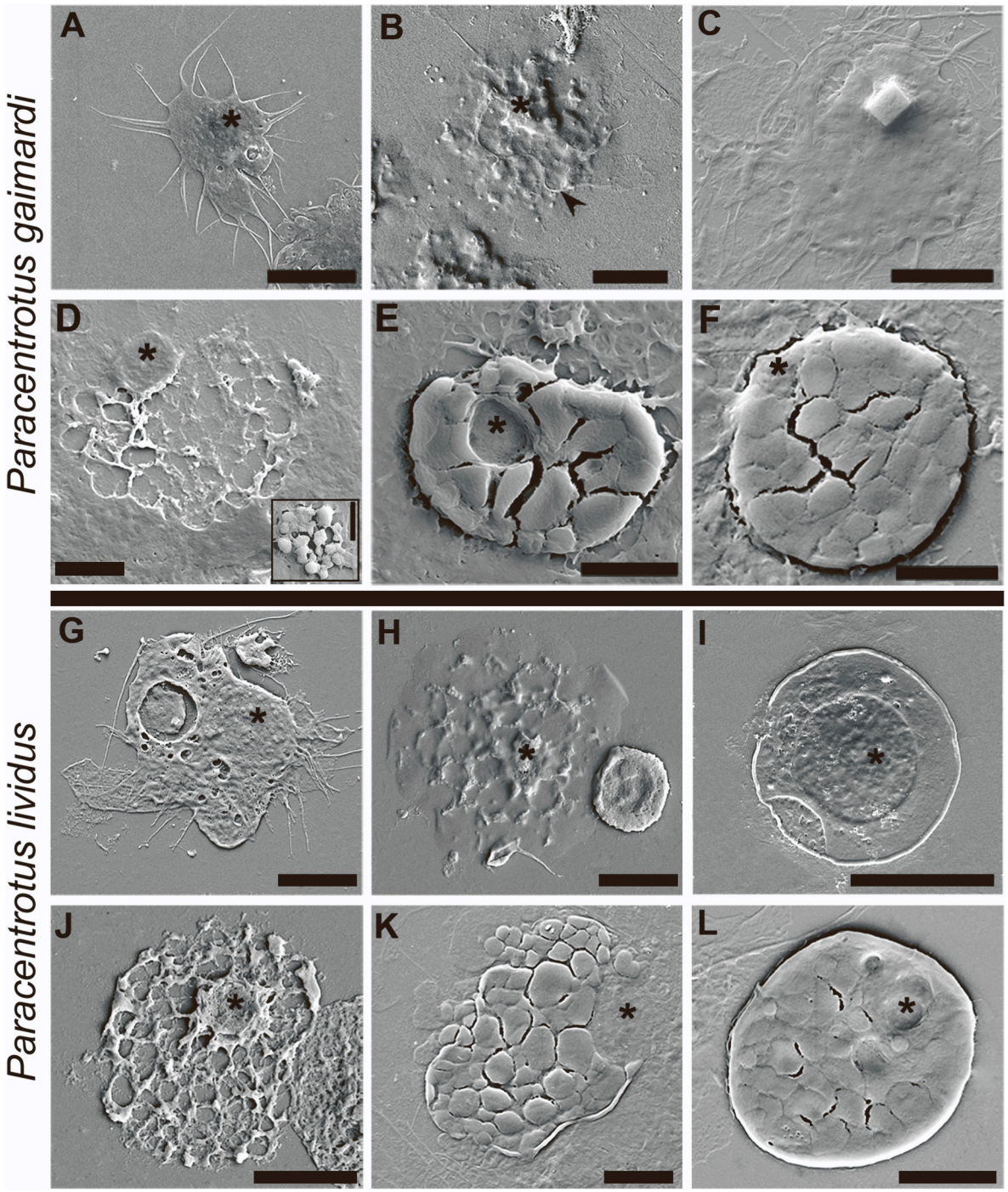

Fig. 2. Scanning electron microscopy of mature coelomocytes in *Paracentrotus* sea urchins. A-F – coelomocytes of *P. gaimardi*; G-L – coelomocytes of *P. lividus*. A and G – Phagocyte; B and H – Vibratile cell; C – Crystal cell; I – Progenitor cell; D and J – Red spherulocyte; D *inset* – Typical mature Red spherulocyte; E and K – Colorless spherulocyte; F and L – Granular spherulocyte. Arrowhead = Flagellum; Asterisk = nucleus. Scale: A = 10 μm; B-L = 5 μm.

filiform or bladder-like cytoplasmic expansions and a large nucleus (Fig. 2A and G). Vibratile cells had a pronounced and usually central nucleus and a very spread cytoplasm. Unlike other cells with spherules, vibratile cells seem to be much fragile, losing spherule integrity and becoming much spread (Fig. 2B and H). The flagellum can be occasionally observed (Fig. 2B), but it is easily lost during preparations (Fig. 2H). Crystal cells showed a very spread cytoplasm, with no visible nucleus and a remarkable cubic crystalloid beneath a thin layer of the cell membrane (Fig. 2C). Progenitor cells are flat and round, with a large central nucleus surrounded by a thin layer of cytoplasm (Fig. 2I).

Red spherulocyte showed a remarkable thicker nucleus and a very flattened cytoplasm (almost spread), composed of a lattice of large and uniform spaces that contained the spherules (Fig. 2D and J). Though very difficult to find in SEM preparations, typical mature red spherulocytes exhibited round, loosely grouped, regular-sized spherules (Fig. 2D *inset*). By contrast, colorless and granular spherulocytes showed a comparatively thicker cell, with well-delimited spherules of irregular sizes and shapes in colorless spherulocytes (Fig. 2E and K), or regular sizes and shapes in granular spherulocytes (Fig. 2F and L).

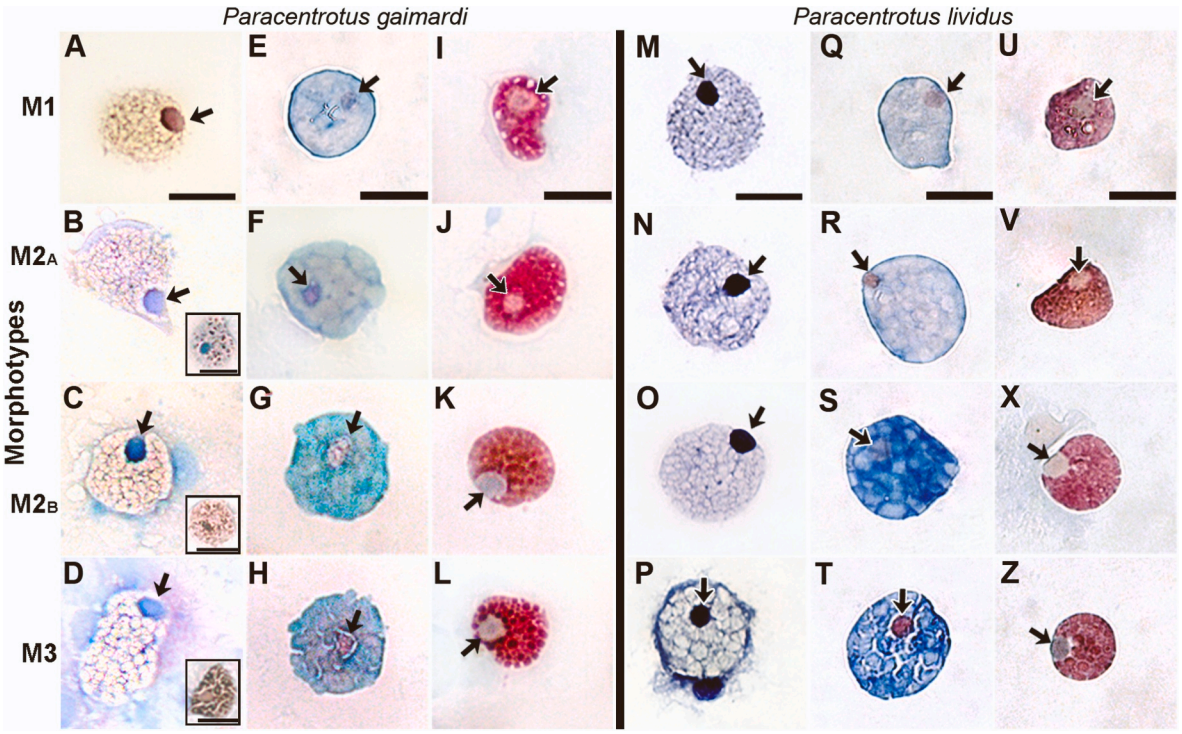

Fig. 3. Different morphotypes (M1 to M3) of the spherulocytes of *Paracentrotus* sea urchins. A-L – Spherulocytes of *P. gaimardi*; M-Z – Spherulocytes of *P. lividus*. A-D and M–P – Red spherulocyte; E-H and Q-T – Colorless spherulocyte; I-L and U-Z – Granular spherulocyte. A, E, I, M, Q, and U – Morphotype 1; B–C, F-G, J-K, N–O, R–S, V-X – Morphotype 2; D, H, L, P, T, Z – Morphotype 3. A-L and Q-Z – Mallory's trichrome; M–P – Toluidine blue. Scale: 10 μm. Arrow = nucleus. (For interpretation of the references to colour in this figure legend, the reader is referred to the Web version of this article.)

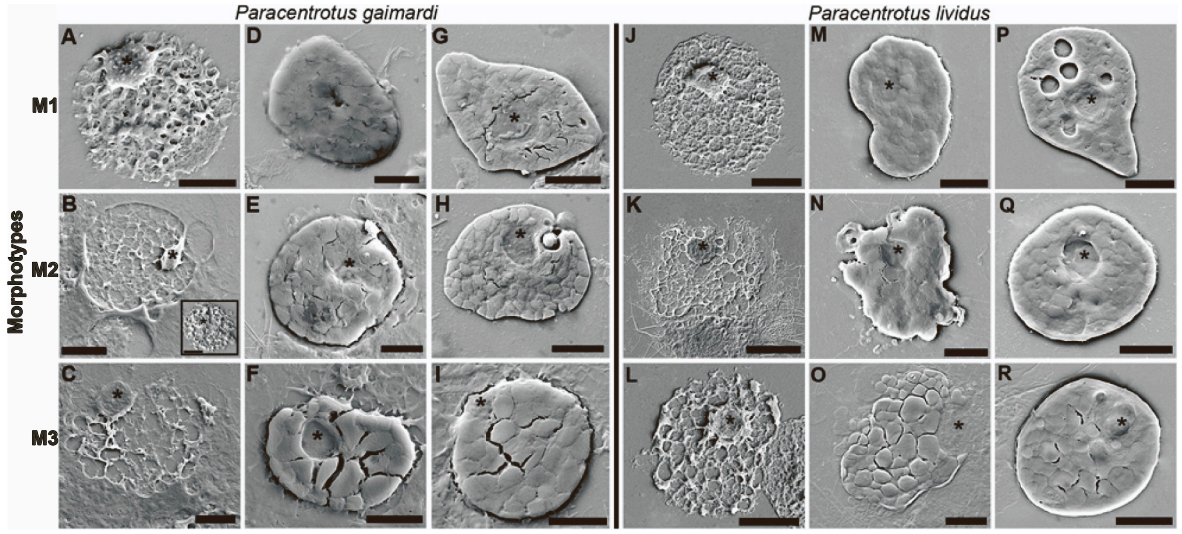

Fig. 4. Scanning electron microscopy of different morphotypes (M1 to M3) of the spherulocytes in *Paracentrotus* sea urchins. A-I – Spherulocytes of *P. gaimardi*; J-R – Spherulocytes of *P. lividus*. A-C and J-L – Red spherulocyte; D-F and M–O – Colorless spherulocyte; G-I and U-Z – Granular spherulocyte. A, D, G, J, M, and P – Morphotype 1; B, E, H, K, N, and Q – Morphotype 2; C, F, I, L, O, and R – Morphotype 3. Scale: A-J and L-R = 5 μm; K = 10 μm. Asterisk = nucleus. Due to the scarcity of good scanning electron microscopy pictures, photographs of M3 for both species are the same used to illustrate mature spherulocytes in Fig. 3.

3.4. Morphology and morphometry of different morphotypes of spherulocytes

A set of similar morphotypes was found within all spherulocyte subpopulations in both species (Figs. 3, 4 and 6), and named morphotypes 1, 2, and 3 (M1, M2, and M3). Morphological analyzes showed that morphotypes belonging to the same spherulocyte subpopulation were in general similar, but presented small differences related to the nuclear dimensions and cytoplasmic organization (Figs. 3 and 4). The morphotypes were cytochemically similar, differing sometimes in the intensity of the stain (Fig. 3F, G, R, and S). Nucleus color in MT preparations also differed between morphotypes of the same cell (Fig. 3), which can be interpreted as a physiological variation (Wołuń-Cholewa et al., 2010). Measurements were consistently different among the morphotypes, showing that nucleus diameter and N/C ratio were the largest in cells in M1, decreasing in M2, being the smallest in M3 (Fig. 6; Supplementary Table 1). By contrast, cytoplasm diameter was similar in all morphotypes (Fig. 6; Supplementary Table 1). Statistical analyzes

Table 1
Total and differential cell counts in *Paracentrotus* sea urchins.

Parameters	*Paracentrotus gaimardi*	*Paracentrotus lividus*
Total cell count (cell/mL)	$5.53 \times 10^6 \pm 5 \times 10^5$	$5.35 \times 10^6 \pm 5.75 \times 10^5$
Differentia cell count (%)		
Phagocytes	77.8 ± 1.8	81.9 ± 4.1
Vibratile cells	5.8 ± 1.46	7.74 ± 2.47
Red spherulocyte	10 ± 0.45[a]	5.03 ± 1.34
Colorless spherulocyte	6.39 ± 0.85	5.33 ± 0.91
Crystal cell	>1	–
Progenitor cell	–	>1

Abbreviations: a = Significant differences in Student t-test between species ($p < 0.05$).

showed that the cytoplasm diameter of all spherulocytes (except red spherulocytes) was affected by the species considered, while morphotype and the interaction of these factors did not affect this parameter (Supplementary Table 2). By contrast, nucleus diameter and N/C ratio were usually affected by morphotype and species (except red spherulocytes), while the interaction of these factors (except in colorless spherulocytes) did not affect them (Supplementary Table 2).

In M1, red spherulocytes are compact cells with a prominent peripheral nucleus (Fig. 3A and M; Fig. 4A and J), presenting the largest diameter and N/C ratio (Fig. 6A and C; Supplementary Table 1). The cytoplasm has an unorganized and empty mesh composed of finely reticulated spaces (Fig. 3A and M; Fig. 4A and J), and its diameter was stable during all the processes (Fig. 6B). In M2 as a whole (*i.e.* M2A and M2B), the nucleus stays prominent (Fig. 3B, C, N, and O; Fig. 4B and K), but the diameter and the N/C ratio decrease if compared to the previous morphotype (Fig. 6A and C; Supplementary Table 1). The lattice in the cytoplasm of M2 cells becomes more organized than in M1, being composed of elongated and round small spaces (*i.e.* M2A – Fig. 3B and N; Fig. 4B and K), or only small round spaces (*i.e.* M2B – Fig. 3C and O). However, the cytoplasm diameter is similar to the previous stage (Fig. 6; Supplementary Table 1). On some rare occasions, the cytoplasm may be covered by a granular material with a brownish coloration in MT preparations (Fig. 3B and C *insets* and Fig. 4B *inset*), most likely echinochrome. In the M3, red spherulocytes show the smallest nucleus diameter, along with the largest N/C ratio (Fig. 6A and C; Supplementary Table 1). The cytoplasmic lattice presents large round and more regular inclusions (Fig. 3D and P; Fig. 4C and L), that may be covered with a granular material in *P. gaimardi* (Fig. 3D *inset*).

The spherule content of red spherulocytes is very sensitive to cytological procedures, in special in *P. lividus*, which prevented us to find typical mature cells (Fig. 1J and V). However the overall organization is maintained and the cell type can be easily identified also in stained and SEM preparation. It was common to find empty red spherulocytes in both species (Fig. 4A–C and J-L), but with a peculiar cytoplasmic organization, ranging from small to large cytoplasmic reticules (Fig. 3A–D and M–P). After careful analyses, we observed that different spherule diameters could be related to specific morphotypes. There is a strong negative correlation between spherule diameter and nucleus size (*P. gaimardi*: r = - 0.742, p = 0.0001; *P. lividus*: r = - 0.715; $p < 0.0001$), indicating that the spherules increase while nuclei become more condensed (Fig. 6A and B). Additionally, the spherule diameters of red spherulocytes differed among morphotypes (Fig. 7C). Spherule diameter was not affected by species (F = 0.274; p = 0.6011), while morphotypes

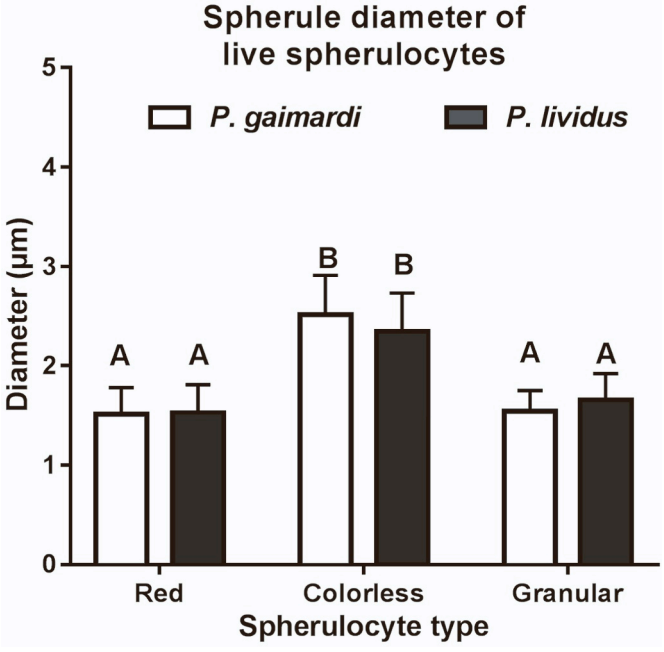

Fig. 5. Diameter of spherules in live spherulocytes in *Paracentrotus* sea urchins. Different letters indicate significant differences ($p < 0.05$) among cell types in two-way ANOVA analyses. Error bars represent the standard deviation of the mean.

Table 3
Diameter, in µm, of cytoplasmic spherules of live red, colorless and granular spherulocytes.

Cell type	*Paracentrotus gaimardi*	*Paracentrotus lividus*
Red spherulocyte	1.51 ± 0.27 [A]	1.52 ± 0.29 [A]
	1.06–2.10	1.09–2.18
Colorless spherulocyte	2.51 ± 0.40 [B]	2.34 ± 0.39 [B]
	1.94–3.34	1.72–3.05
Granular spherulocyte	1.54 ± 0.21 [A]	1.65 ± 0.27 [A]
	1.20–1.95	1.16–2.50

Measurements are expressed as mean ± standard deviation (M ± SD), followed by range (Min-Max).
Capital letters indicate significant differences in spherule size among different cell types.

Table 2
Diameter of the cytoplasm and nucleus (in µm) of coelomocytes for *Paracentrotus gaimardi* and *Paracentrotus lividus*.

Cell Types	*Paracentrotus gaimardi*				*Paracentrotus lividus*			
	Live		Stained		Live		Stained	
	Cytoplasm	Nucleus	Cytoplasm	Nucleus	Cytoplasm	Nucleus	Cytoplasm	Nucleus
Phagocytes	17.6 ± 4.81	4.49 ± 0.66	21.95 ± 4.48	6.95 ± 0.54	24.54 ± 4.01	5.71 ± 1.72	17.78 ± 5.29	5.21 ± 0.83
Vibratile cells	7.62 ± 1.03	4.11 ± 0.47	13.71 ± 0.73	4.31 ± 0.50	9.38 ± 0.59	3.92 ± 0.59	14.31 ± 0.80	4.50 ± 0.42
Crystal cell	5.08 ± 0.32	a	6.03 ± 0.34	a	b	b	b	b
Progenitor cell	b	b	b	b	6.51 ± 0.67	4.43 ± 0.39	5.85 ± 0.30	4.48 ± 0.54
Red spherulocyte[c]	9.47 ± 0.86	3.61 ± 0.57	13.60 ± 1.92	3.46 ± 0.70	10.66 ± 1.31	3.36 ± 0.21	14.79 ± 1.95	3.39 ± 0.27
Colorless spherulocyte[c]	11.69 ± 1.5	4.21 ± 0.30	15.01 ± 2.04	3.11 ± 0.60	13.95 ± 1.35	5.08 ± 0.73	17.53 ± 3.73	3.32 ± 0.63
Granular spherulocyte[c]	8.96 ± 0.84	3.95 ± 0.45	13.85 ± 1.25	4.20 ± 0.67	9.30 ± 0.93	3.36 ± 0.52	11.90 ± 1.46	3.09 ± 0.48

Measurements are expressed as mean ± standard deviation (M ± SD).
Abbreviations: a = nucleus not observed; b = cell not found; c = measurements made in cells at morphotype 3 (M3).

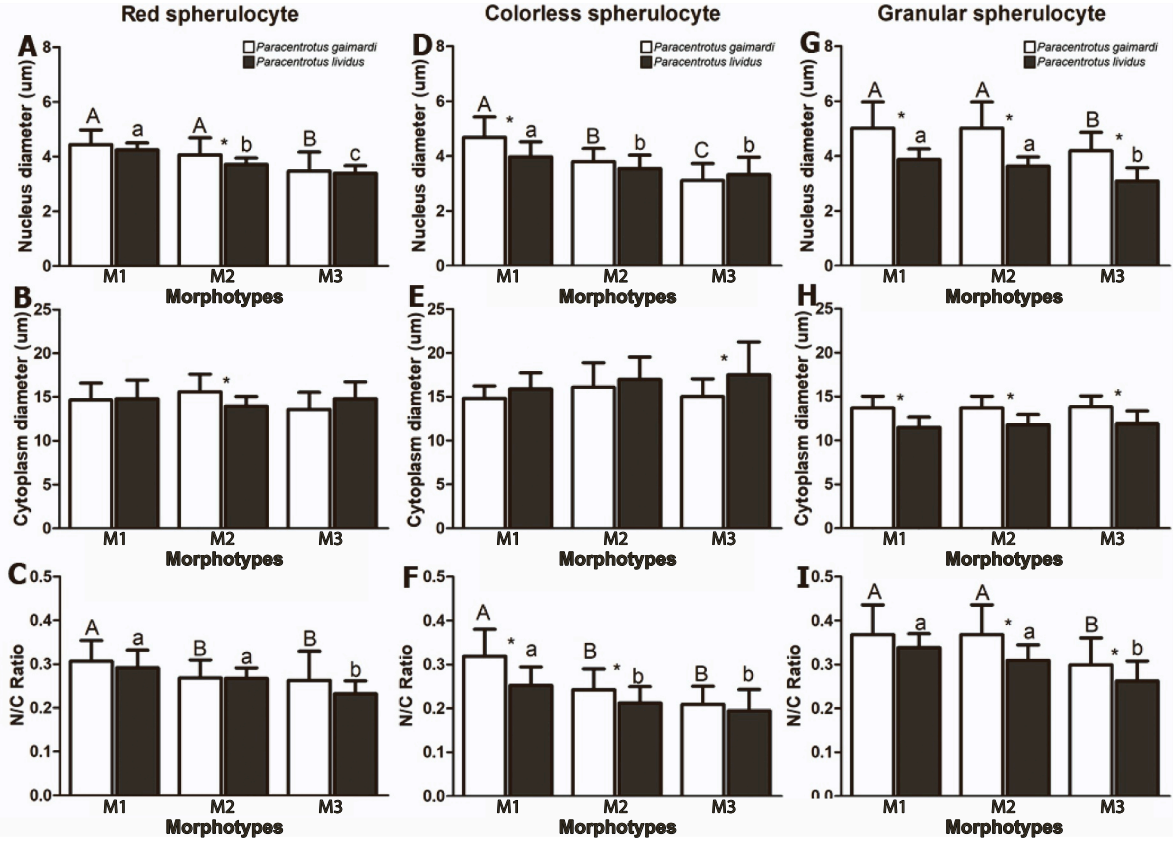

Fig. 6. Morphometry of different morphotypes (M1 to M3) of spherulocytes in *Paracentrotus* sea urchins. A, D, and G – Nucleus diameter; B, E, and H – Cytoplasm diameter; C, F, and I – Nucleus/Cytoplasm Ratio. Capital letters – *P. gaimardi*, Small letters – *P. lividus*. For each parameter, distinct letters show significant differences among stages ($p < 0.05$), with uppercase to *P. gaimardi* and lowercase to *P. lividus*. Asterisk (*) shows significant differences between species ($p < 0.05$). Legend: N/C ratio = Nucleus/Cytoplasm Ratio.

($F = 285.2$; $p < 0.0001$), and the interaction of these two factors ($F = 4.326$; $p < 0.0142$) affected the cytoplasm diameter. The M1 of the red spherulocyte (Fig. 3A and M) exhibited a reticulated and unorganized cytoplasm with very small spherules (0.58 ± 0.13 μm in *P. gaimardi*; 0.64 ± 0.12 μm in *P. lividus*), while cells identified as M2 showed a mix of elongated and round small areas, or cells with only small round areas (*i.e.* M2A and M2B respectively – Fig. 3B and N; Fig. 3C and O). The M2 cells measured 0.95 ± 0.25 μm in *P. gaimardi* and 1.05 ± 0.13 μm in *P. lividus* (Fig. 7C). The cytoplasm in M3 red spherulocytes showed a uniformly organized lattice composed by large round-shaped spaces (Fig. 4D and P), with a diameter of 1.61 ± 0.30 μm in *P. gaimardi* 1.5 ± 0.31 μm in *P. lividus*. These differences were significant among morphotypes in the same species, but not between species (Fig. 7C).

The colorless spherulocytes followed the same general pattern seen in the red ones (Fig. 6) since the nucleus and the N/C ratio were larger in M1 (Fig. 6D and F; Supplementary Table 1). However, differently from the red ones, colorless spherulocytes have a uniformly homogeneous cytoplasm formed by discrete divisions (Fig. 3E and Q; Fig. 4D and M). Colorless spherulocytes in M2 present a smaller nucleus if compared to early-stage cells (Fig. 6D) and its n/c ratio is also small (Fig. 5F). Although the cytoplasm still looks homogeneous in M2A cells, it is possible to see some early formed spherules (Fig. 3F and R; Fig. 4N), which is more evident in M2B cells (Fig. 3G and S; Fig. 4E). The heterogeneous size of the spherules is already visible in cells at M2 (Fig. 3F, G, R, and S; Fig. 4E and N). The M3 of the colorless spherulocytes showed the smallest nucleic size and N/C ratio (Fig. 6D and F; Supplementary Table 1), and the nucleus is remarkably visible since it is usually seen as a depression in the cytoplasm (Fig. 4F and O). The cytoplasm is completely formed in M3 cells, and the unequal size of the spherules is remarkable (Fig. 3H and T; Fig. 4F and O). Cytoplasm diameter was similar in all morphotypes (Fig. 6E).

The granular spherulocytes showed a very similar pattern compared to colorless spherulocytes. Their nucleus diameter and N/C ratio were the largest in M1 cells (Fig. 6G and I; Supplementary Table 1), and the cytoplasm also showed the same pattern observed in colorless spherulocytes, being homogeneous with a finely granular appearance (Fig. 3I and U). Still, whitish spots are commonly observed in M1 cells (Fig. 3I and U). SEM analysis showed that although the cytoplasm presents discrete divisions (Fig. 4G and P), the homogeneous appearance can be easily observed, and the white spots in cytochemical preparations are empty holes in the cytoplasm (Fig. 4P). The M2 granular spherulocytes have an intermediate-sized nucleus and nucleus/cytoplasm ratio (Fig. 6G and I; Supplementary Table 1), and the nucleus may be seen as a depression in the cell (Fig. 4H and Q). The cytoplasm begins to be subdivided, and the spherule outline becomes progressively more evident (Fig. 3J, K, V, and X; Fig. 4H and Q). In M2A cells, small homogeneous roundish spherules are already visible (Fig. 3J, V, and 4H), and they become larger in M2B (Fig. 3K, X, and 4Q). Lastly, in M3 cells, the nucleus is quite condensed and has the smallest diameter and nucleus/cytoplasm ratio (Fig. 6G and I; Supplementary Table 1). The cytoplasm bears large uniform-sized spherules (Figs. 3L and Z; Fig. 4I and R). Cytoplasm diameter was similar among morphotypes (Fig. 6H), but the nucleus and cytoplasm diameters and nucleus/cytoplasm ratio differed between species (Fig. 6G–I).

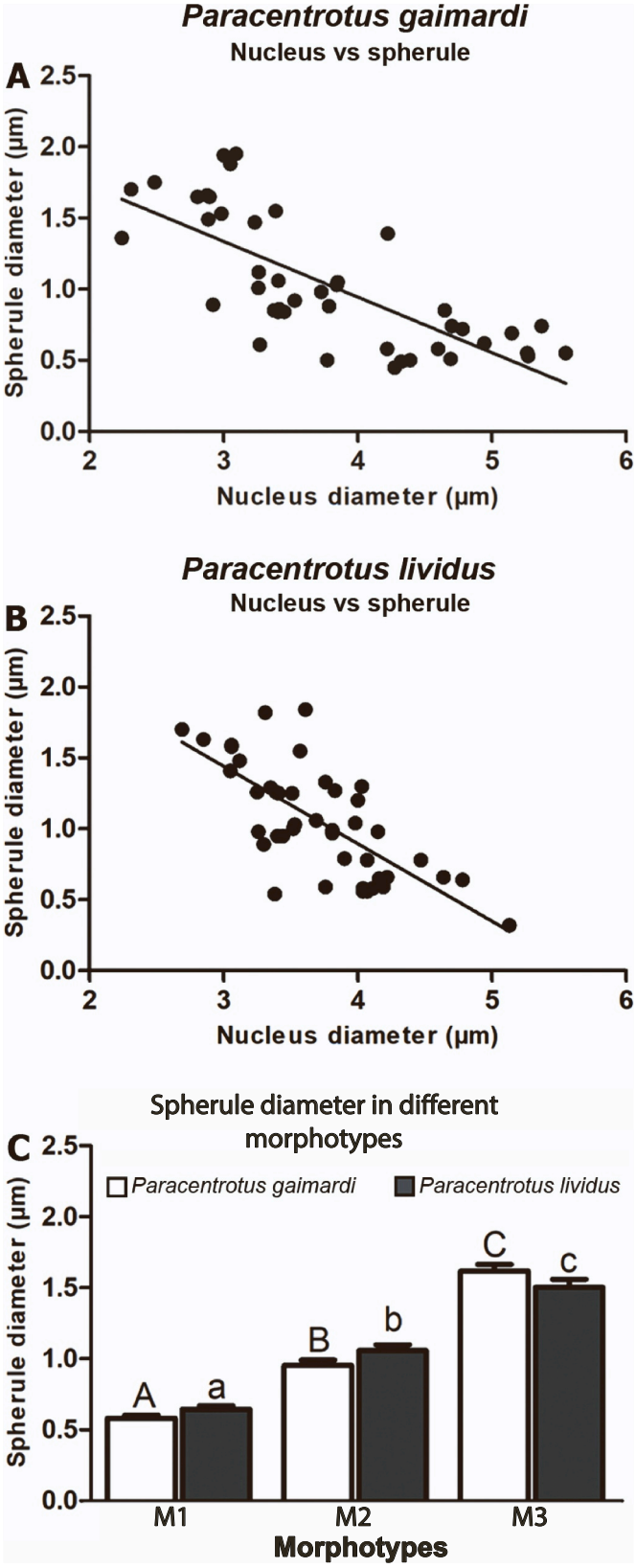

Fig. 7. Spherule diameter of stained red spherulocytes in *Paracentrotus* sea urchins. A and B – Pearson correlation between nucleus diameter and spherule diameter in *P. gaimardi* and *P. lividus* respectively. C – Comparison of spherule diameter in different morphotypes (M1 to M3) *P. gaimardi* and *P. lividus*. Capital letters – *P. gaimardi*, Small letters – *P. lividus*. Distinct letters show significant differences among morphotypes ($p < 0.05$).

4. Discussion

4.1. Paracentrotus coelomocytes and the identification of coelomic cells in other echinoids

From an immunological perspective, *P. lividus* is a relatively well-known species. Although studies on its humoral components are not uncommon (*e.g.* Stabili et al., 1996; Chiaramonte et al., 2020), investigations on its cellular effectors are more frequent (*e.g.* Arizza et al., 2007; Chiaramonte et al., 2019). By contrast, the immune aspects of *P. gaimardi* are completely unknown. In the present study, through a comparative evaluation of the coelomocytes in both species, we observed that their cells are similar. However, the number of subpopulations was underestimated since six cell types were revealed in both species. For the first time, we provided information on the coelomocytes of *P. gaimardi*, as well as a detailed characterization of red, colorless, and granular spherulocytes in both species, including the identification of a set of different morphotypes.

Total and differential cell counts in *P. lividus* were similar to those found in *P. gaimardi* and fit the pattern previously described for echinoids in the literature (Bertheussen and Seljelid, 1978; Smith et al., 2010). Even for the red spherulocytes, which showed a higher percentage in *P. gaimardi*, the proportions are in line with the pattern already observed in *P. lividus* and other sea urchins (Smith et al., 2010). Different factors have been pointed out as capable of influencing physiological or immune parameters, such as gender, age, or symbiotic associations (McCaughey and Bodnar, 2012; Arizza et al., 2013; Queiroz, 2020a); the last two being able to affect cell counts (McCaughey and Bodnar, 2012; Queiroz, 2020a). Thus, the difference observed in the red spherulocyte percentage can be related to factors other than interspecific differences.

Both species presented six cell types, unlike the four usual commonly described types in the literature (*i.e.* phagocytes, vibratile cells, and red and colorless spherulocytes – Branco et al., 2013; Chiaramonte et al., 2019; Work et al., 2020). Phagocytes and vibratile cells are easily identified in fresh or stained preparations, regardless of the approach, due to the presence of prominent cytoplasmic expansions (filiform or bladder-like), or a flagellum, respectively (Work et al., 2020; Queiroz et al., 2021a; 2021b). Petaloid and filopodial phagocytes, which have been pointed out as transitory stages of the same cell type in Echinodermata (Eliseikina and Magarlamov, 2002; Matranga et al., 2005), were common in fresh and stained preparations in our study. For phagocytes, regardless of the stage, morphological features seem to be sufficient to identify this population, as observed here in *Paracentrotus* and other species elsewhere, such as *Tripineuste gratilla*, *E. tribuloides*, *L. variegatus*, *E. lucunter,* and *A. lixula* (Work et al., 2020; Queiroz et al., 2021b). In the case of vibratile cells, the flagellum is very sensitive to handling/fixation, being easily lost during preparation. Nevertheless, we observed that even after losing the flagellum, vibratile cells can be promptly identified in cytological preparations by using the TB stain. They are the only cell type in sea urchins that displays β-metachromasia (purple color) after staining. This reaction was verified herein for both *Paracentrotus* species, and previously for *E. tribuloides*, *E. lucunter*, *L. variegatus*, and *A. lixula* (Queiroz et al., 2021b). An apparent purple coloration was also observed in TB-stained preparations in *P. lividus* (Deveci et al., 2015) and *Strongylocentrous purpuratus* (Holland et al., 1965).

Though crystal cells are considered typical coelomocytes in sea cucumbers (*e.g.* Hetzel, 1963), we provide the first record of a crystal cell in sea urchins. The crystalloid inside sea cucumber crystal cells dissolves under slight osmotic stress or staining procedures (Hetzel, 1963; Queiroz et al., 2022). By contrast, the crystalloid in *P. gaimardi* cells was proven resistant to staining and SEM procedures in our study. This higher resistance suggests that the crystal present in the cells in *P. gaimardi* probably has a different composition from those found in holothuroids. Though they were already recorded in the echinoid *Echinus esculentus*

(Smith, 1981), progenitor cells are commonly observed in holothurians and asteroids (Smith, 1981; Vazzana et al., 2015). The progenitor cell observed in the present study was morphologically similar to progenitor cells observed in *E. esculentus,* in the sea star *Marthasterias glacialis*, and other holothurians (Hetzel, 1963; Vazzana et al., 2015; Caulier et al., 2020; Andrade et al., 2021). A morphologically similar cell, named small cell, was described in *P. lividus* (Deveci et al., 2015), and fits the morphology of the progenitor cell observed here. However, crystal and progenitor cells may be widespread in this genus. They were very rare in the coelomic fluid, which may have hindered finding them in both species. Consequently, both species may have seven cell types, instead of six.

We observed that morphology, morphometry, and stain affinity were essential for the unequivocal identification of red, colorless, and granular spherulocytes in live and stained preparations. All spherulocytes of *P. gaimardi* and *P. lividus* were morphologically and/or cytochemically similar to those of *E. tribuloides*, *E. lucunter*, *L. variegatus, Arbacia punctulata,* and *A. lixula* in MT preparations (Liebman, 1950; Queiroz and Custódio, 2015; Queiroz et al., 2021b). Even analyzed through different methods, the morphology of living and stained red and colorless spherulocytes in *Paracentrotus* sea urchins were quite similar to those of *T. gratilla* (Work et al., 2020). Distinguishing colorless and granular spherulocytes in live preparations can be difficult since both are transparent spherule-filled coelomocytes. Still, accurate analysis of the shape and size of the spherules proved to be enough for identification. A similar situation may be seen in *A. punctulata* since "green and red threphocytes" have similar-sized spherules, while the "colorless threphocytes" spherules are large and irregular (Liebman, 1950). By contrast, we had no problems in identifying the three different spherulocytes in MT-stained preparations. While red spherulocytes show either brownish spherules or an uncolored and empty cytoplasm (probably due to the removal of their content during slide preparation), colorless and granular spherulocytes are quite different since they stain blue and pink respectively (Cf. Fig. 3). These differences indicate the predominance of (proteo)glycans in the colorless spherulocytes, while the granular ones present a peptidic moiety. Although the specific chemical identity of these compounds needs further studies by more precise chemical methods, this clearly shows different physiological functions for these cell types. Colorless trephocytes of *A. punctulata* also stained blue in MT preparations (Liebman, 1950). Additionally, the newly-described granular spherulocyte (Queiroz and Custódio, 2015) may be easily identified in TB preparations because this spherulocyte is the only one that becomes grayish after staining (*Cf.* Fig. 1X *inset* and Supplementary Fig. 1).

We obtained detailed structural information for *Paracentrotus* coelomocytes through SEM analysis, confirming all morphological features observed in cytological preparations. Morphological aspects were quite specific for each cell type, and based on these characteristics, the coelomocytes could be divided into two main groups: non-spherulous and spherulous cells. Phagocytes, crystal, and progenitor cells fall within the first group. Crystal cells are easily identified due to the conspicuous crystalloid, while phagocytes and progenitor cells may be distinguished according to specific sizes and cytoplasmic complexity. The second group can be further divided into (1) cells with flattened or spread cytoplasm and a thicker nucleus; and (2) cells with thicker cytoplasm and depressed nucleus. Although vibratile cells and red spherulocytes share some characters with the first subgroup, the very spread cytoplasm of vibratile cells and the empty reticulated cytoplasm in red spherulocytes allow for accurate identification. Colorless and granular spherulocytes are in the second subgroup and can be distinguished according to their cytoplasmic spherules, which are large and heterogeneous in colorless spherulocytes, and smaller and homogeneous in granular spherulocytes.

Although the present work is focused on *Paracentrotus*, it certainly may be useful to identify coelomocytes in other sea urchins, in both live, stained, and SEM preparations, as observed for *E. tribuloides*, *E. lucunter*, *L. variegatus, A. punctulata, A. lixula,* and *T. gratilla* (Liebman, 1950; Queiroz and Custódio, 2015; Work et al., 2020; Queiroz et al., 2021b). In the case of phagocytes, vibratile cells, progenitor cells, and crystal cells, they are different enough not to be confused. Still, the main characteristics of each type (*e.g.* cytoplasmic expansion of phagocytes, the flagellum of vibratile cells, the huge nucleus of progenitor cells, and the remarkable crystalloid of crystal cells) were seen in different types of preparation (*Cf.* Figs. 1 and 2). For spherulocytes, the situation is somewhat different. Except for some of our previous works (Queiroz and Custódio, 2015; Queiroz et al., 2021b), which detailed the granular spherulocyte, all other studies addressing sea urchin coelomocytes describe only red and colorless spherulocytes (*e.g.* Branco et al., 2014; Romero et al., 2016; Work et al., 2020). However, the present work provides a set of morphological, morphometric, and cytochemical characteristics that can be used to accurately differentiate red, colorless, and granular spherulocytes in *Paracentrotus.* Some of these features were already observed in other species (*e.g. E. tribuloides*, *E. lucunter, L. variegatus, A. lixula,* and *A. punctulata* – Liebman, 1950; Queiroz and Custódio, 2015; Queiroz et al., 2021b). We also confirm that cytocentrifugation may be quite useful to study echinoderm coelomocytes, as previously demonstrated by successful results in asteroids, holothuroids, and echinoids (Taguchi et al., 2016; Queiroz and Custódio, 2015; Queiroz et al., 2021b; Queiroz et al., 2022).

4.2. Insights on spherulocytes morphotypes and implications to sea urchin physiology

The main aspects of vertebrate blood cells have long been unraveled, including the cell types, their functions, as well as their maturation process (Turgeon, 2012; Campbell, 2015). The knowledge is so extensive that markers for differ maturation stages were already identified since the 90s (Terstappen et al., 1990). Neutrophils provide a good example of how the maturation process of vertebrate blood cells is widely clarified since both morphological and molecular aspects of each stage are known for this immune cell (Bessis, 1977; Lawrence et al., 2018). By contrast, the situation for invertebrates is quite different and, except for a few groups (*e.g.* insects and ascidians), the knowledge of invertebrate coelomocytes/hemocytes is considerably scarcer. In general, molecular markers for invertebrates are limited and usually unable to differentiate cell types (*e.g.* Dyrynda et al., 1997), and this also applies to echinoderms (*e.g.* Lin et al., 2007). Consequently, most studies with invertebrates still use morphological features to examine hemocyte/-coelomocyte maturation (Cheng and Guida, 1980; Fontaine and Hall, 1981; Battison et al., 2003; Rebelo et al., 2013).

The data provided here demonstrate that knowledge about spherulocytes is still limited. In addition to finding a new subpopulation in one of the most studied species of the phylum (*i.e. P. lividus*), a set of different morphotypes was observed in each spherulocyte subpopulation. We observed that the cytoplasmic characteristics of all spherulocytes were within a continuum: at one end, cells with homogeneous or finely reticulated cytoplasm (M1) and at the other one, cells with completely formed spherules (M3. *Cf.* Fig. 3). Posteriorly, morphometric analyzes confirmed that nucleus diameter, N/C ratio, and spherule diameter (in red spherulocytes) could be inversely correlated with cytoplasmic alterations, and all these aspects were confirmed by SEM analyses.

Even after obtaining all this data on morphology, morphometry, and cytochemistry for spherulocytes, one important question remains: what do these similar morphotypes mean? Based on our data, we believe that this set may represent distinct stages of a maturation process. In this context, we hypothesize that 'immature' spherulocytes (M1 cells) show a large nucleus, a homogeneous cytoplasm filled by very small spherules (easily observed in the red spherulocyte), as well as a high N/C ratio. As the spherules become larger, the nucleus becomes more condensed and the N/C ratio decreases, as seen in M2A and M2B. The process culminates in 'mature' spherulocytes (M3), with the most condensed nucleus,

and consequently the smallest nuclear diameter, the lowest nucleus/cytoplasm ratio, and cytoplasm filled with large and well-organized spherules. A schematic diagram of this hypothesis is presented in Fig. 8.

Assuming our hypothesis is correct, three questions arise. The first one is why do we believe this is a maturation process? The decrease of nuclear dimensions, and consequently of nucleus/cytoplasm ratio, has long been understood as predictors of cell maturation (Nieburgs, 1967; Bainton, 1988; Turgeon, 2005). Such process is well documented in neutrophils (Bessis 1977; Bainton 1988) in which the nuclear dimensions of early developmental stages, such as promyelocytes, are larger than that observed in mature stages – *e.g.* segmented neutrophils (Bessis, 1977; Bainton 1988). Additionally, nuclear size can be seen from a functional perspective, being positively correlated with RNA synthesis (Baluska and Kubica, 1987; Sato et al., 1994) and transcriptional regulation (Grosch et al., 2020). Such a scenario compares well with the sequence proposed here. In immature spherulocytes, the larger nucleus and the homogeneous cytoplasm – which seem to indicate a large number of small spherules, as observed in an ultrastructural study of the granular spherulocyte of *E. tribuloides* (*Cf.* Queiroz and Custódio, 2015 - Fig. 8) – may be correlated with higher RNA synthesis aimed at generating the content of the spherules. As the process goes on and the spherules are being formed, the nucleus decreases in size, culminating in the smallest nucleus diameter and the largest spherule sizes (as measured here in red spherulocytes), suggesting that high rates of RNA synthesis are no longer needed.

The second question is related to the presence of spherules, with immature spherulocytes having no spherules or smaller ones, and mature spherulocytes having larger spherules. This idea stems from previous studies with invertebrates and vertebrates, and the maturation process hypothesized here for *Paracentrotus* spherulocytes follows the general pattern previously observed in other species. In the sea urchin *E. tribuloides*, the nucleus size of red, colorless, and granular spherulocytes decreased in parallel with the maturation process (Queiroz and Custódio, 2015). A similar tendency was observed in the acidophilic spherulocyte of *Holothuria grisea, H. arenicola,* and *Holothuria tubulosa* (Queiroz et al., 2022), and for morula cells in *Apostichopus japonicus*, *Cucumaria japonica*, and *H. leucospilota* (Endean, 1958; Eliseikina and Magarlamov, 2002). In the first study, the authors observed that morphotype 1 cells (similar to our M1) showed the largest nucleus diameter and nucleus/cytoplasm ratio, while morphotype 4 cells (similar to our M3) presented the smallest nucleus diameter and nucleus/cytoplasm ratio (Queiroz et al., 2022). In the latter two (Endean, 1958; Eliseikina and Magarlamov, 2002), the authors stated that "immature cells" show large nuclei and few/no spherules; while "mature cells" showed small nucleus and a cytoplasm crowded of spherules. Morphological alterations were also observed in hemocytes of the mollusks *Crassostrea rhizophorae* and *Bulinus truncate*, and in the crustaceans *Homarus americanus* (Cheng and Guida, 1980; Battison et al., 2003; Rebelo et al., 2013). For *B. truncate* and *H. americanus*, the chromatin was more condensed and organized in mature cells (Cheng and Guida, 1980; Battison et al., 2003; Rebelo et al., 2013), and the N/C ratio was also high in immature hemocytes of *H. americanus* (Battison et al., 2003). In the study by Li et al. (2021), which used the crustacean *Cherax quadricarinatus*, the authors combined molecular, cellular, and physiological evidence to describe the entire maturation process of granular cells (the equivalent of sea urchin spherulocytes). They found that immature hemocytes present a large nucleus and few/no cytoplasmic granules, while mature hemocytes present a small nucleus and a cytoplasm full of large granules (Li et al., 2021 – Fig. 8). Morphological changes during cell maturation were also reported for vertebrates. Similar changes in the nucleus were observed in mammalian blood cells (Moras et al., 2017; Arpitha et al., 2005; Pethig et al., 2010), and related to the levels of transcriptional activity (Efroni et al., 2008). Thus, although we know that functional evidence on the maturation process of *Paracentrotus* sea urchins is still necessary to confirm our hypothesis, the theoretical framework about other species gives us the confidence to propose that M1 represents immature spherulocytes, while M3 represents mature spherulocytes (Fig. 8).

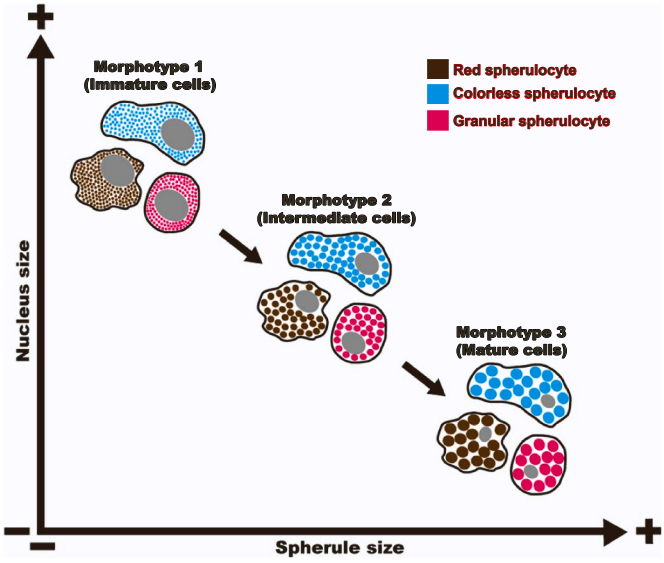

Fig. 8. Schematic representation of the putative processes illustrating the general tendencies during the spherulocytes maturation, as seen by morphological and morphometric features. Immature cells present a large nucleus and an unorganized cytoplasm filled with very small spherules, which give a "smooth" appearance. During the maturation, the nucleus decrease in diameter, and the tiny cytoplasmic spherules fuse, becoming larger. Mature coelomocytes show a smaller nucleus diameter, and the cytoplasm is filled with large spherules. The colors and the shapes of the cells in the picture refer to their color and morphology in Mallory's trichrome. Brown = Red spherulocyte; Blue = colorless spherulocyte; Pink = granular spherulocyte. (For interpretation of the references to colour in this figure legend, the reader is referred to the Web version of this article.)

The third question deals with the origin of the coelomocytes. In Echinodermata, two hypotheses have been proposed to explain the origin of these cells (Matranga et al., 2005). The first one states that coelomocytes would be terminally differentiated cells, which assumes the presence of a hematopoietic organ/tissue. The axial organ has long been proposed as hematopoietic (for review see Matranga et al., 2005), and recent evidence has corroborated this assumption (Golconda et al., 2019). The alternative hypothesis proposes that the coelomic cells would originate from circulating stem cells (*e.g.* progenitor cell – Matranga et al., 2005), and coelomocytes would differentiate into the coelomic fluid. However, only one study with sea urchins has supported this idea (Holland et al., 1965). Regardless of where coelomocytes originate, all different morphotypes were found in the coelomic fluid, suggesting that, at least for spherulocytes, maturation occurs in the coelom. Our results are in line with those observed for the mollusk *C. rhizophorae* and the crustacean *C.quadricarinatus* (Rebelo et al., 2013; Li et al., 2021) since the maturation process of their hemocytes was observed in hemolymph samples.

Based on the present study and the literature available on sea urchins, it is also possible to speculate that granular spherulocytes may be common among regular sea urchins. Considering that it was properly recorded in the orders Cidaroida (*E. tribuloides*), Arbacoida (*A. lixula*), and different families of Camarodonta (*E. lucunter*, *L. variegatus*, *P. gaimardi,* and *P. lividus*), it is plausible to believe that granular spherulocytes are widespread in regular sea urchins. Information on the other cell types is scarce, which limits further discussions. The physiological function of the new/poorly known cell types described here surely deserves further study. While crystal cells are commonly pointed out to be involved in osmoregulation (at least for holothurians – Eliseikina and Magarlamov, 2002), the real function of the progenitor cells (*i.e.* if lymphocytes or proliferative cells – Vazzana et al., 2015; Ho and

Rast, 2016) remains uncertain. In the case of granular spherulocytes, morphological and cytochemical evidence presented here and elsewhere (Queiroz and Custódio, 2015; Queiroz et al., 2021b) suggests that they may be closely related to the acidophilic spherulocytes observed in some holothurians (*e.g. H. grisea, H. arenicola,* and *H. tubulosa* – Vazzana et al., 2015; 2018, Queiroz et al., 2022). Their similar morphology and cytochemistry may suggest that granular spherulocytes are involved in cytotoxic responses in sea urchins, as seen in *H. tubulosa* (Vazzana et al., 2018). However, Arizza et al. (2007) showed that in *P. lividus*, this function is performed by colorless spherulocytes. This aspect deserves to be properly addressed in future studies. Considering the close phylogenetic relationship between *P. gaimardi* and *P. lividus*, as well as the similarity between their immune cells, behavior, and feeding habits (Queiroz, 2020b), it is reasonable to assume that the immunological/-physiological responses of these species should be similar.

5. Conclusion

The presence of only four main types of coelomocytes in sea urchins has been a consensus for decades (Smith, 1981; Smith et al., 2006; 2010; 2018). However, with the discovery of new subpopulations (Queiroz and Custódio, 2015; Queiroz et al., 2021b; present study), the general scenario will certainly change. In addition to characterizing the coelomocytes of *P. gaimardi* for the first time, our data reveal that the number of cells in *P. lividus* was underestimated. Since *P. lividus* is one of the most studied sea urchins in the world, this indicates that data on coelomocytes of other echinoderms (*e.g.* Asteroidea and Holothuroidea) may be inaccurate as well. The maturation process of the spherulocytes also deserves more answers. The integrative approach used here was essential to demonstrate that different morphotypes of the same spherulocyte subpopulation should not be interpreted as different cell types with similar features. Instead, they may be grouped in a logical sequence related to the maturation process. Although this possibility seems attractive, we reinforce the need for further studies with different sea urchin species, and maybe other echinoderms as well, to corroborate our hypothesis.

Our work provides consistent guidelines to identify each type of coelomocyte in *Paracentrotus*, whether in live, cytological, or SEM preparations. Certainly, our results will be useful to identify coelomocytes in other species, as may be observed in *E. tribuloides*, *L. variegatus*, *E. lucunter, A. lixula,* and *T. gratilla* (Work et al., 2020; Queiroz et al., 2021b). This is particularly important regarding live colorless and granular spherulocytes, which can easily be confused due to their similar color and morphology. Nevertheless, we have demonstrated that the shape and size of their cytoplasmic spherules are distinguishable and can be used to tell them apart. Lastly, many aspects unraveled in this study give rise to more specific questions. These questions could guide future studies with a more restricted scope, *i.e.*, addressing sea urchin coelomocytes and immunobiology, or with a wider view, i.e., how to apply these methods to Echinodermata in a broad sense.

Funding

This study was supported by the Fundação de Amparo a Pesquisa do Estado de São Paulo - FAPESP (Grant numbers: 2015/21460-5; 2018/14497-8; 2021/10161-8) and Coordenação de Aperfeiçoamento de Pessoal de Nível Superior-CAPES.

Contribution statement

We also confirm that all named authors contributed to the preparation of the manuscript. **Vinicius Queiroz** performed all analysis, interpreted data, and wrote the manuscript; **Vincenzo Arizza** and **Mirella Vazzana** supervised the development of the work with the Italian species, helped in data interpretation, manuscript preparation, and critical revision; **Márcio R. Custódio** supervised the development of work with the Brazilian species, helped in data interpretation, manuscript preparation, and critical revision.

Declaration of competing interest

The authors declare that they have no known competing financial interests or personal relationships that could have appeared to influence the work reported in this paper.

Acknowledgments

The authors thanks Prof. Renata G. M. Whitton, Prof. José Eduardo A. R. Marian (IB-USP), and Prof. Álvaro Migoto (CEBIMAR-USP), for the support with light microscopy photographs. We also thank Prof. Dr. Alberto Ribeiro and the technicians Sheilla Shumidt and Márcio Cruz for support with electron microscopy imaging. The author is indebted to Daniel C. Cavallari for the English improvements. This work was supported by FAPESP (Proc. 2015/21460-5; 2018/14497-8; 2021/10161-8) and Coordenação de Aperfeiçoamento de Pessoal de Nível Superior (CAPES). This is a contribution of NP-BioMar (Research Center for Marine Biodiversity - USP).

Appendix A. Supplementary data

Supplementary data to this article can be found online at https://doi.org/10.1016/j.jcz.2022.06.008.

References

Alves, M.B., Emerenciano, A.A., Bordon, I.C., Silva, J.R.M., Fávaro, D.I., 2018. Biomonitoring evaluation of some toxic and trace elements in the sea urchin *Lytechinus variegatus* (Lamarck, 1816) in a marine environment: northern coast of São Paulo (Brazil). J. Radioanal. Nucl. Chem. 316 (2), 781–790.

Andrade, C., Oliveira, B., Guatelli, S., Martinez, P., Simões, B., Bispo, C., Ferrario, C., Bonasoro, F., Rino, J., Sugni, M., Gardner, R., Zilhão, R., Coelho, A.V., 2021. Characterization of coelomic fluid cell types in the starfish *Marthasterias glacialis* using a flow cytometry/imaging combined approach. Front. Immunol. 12, 807.

Arizza, V., Giaramita, F., Parrinello, D., Cammarata, M., Parrinello, N., 2007. Cell cooperation in coelomocyte cytotoxic activity of *Paracentrotus lividus* coelomocytes. Comp. Biochem. Physiol. Mol. Integr. Physiol. 147, 389–394. https://doi.org/10.1016/j.cbpa.2007.01.022.

Arizza, V., Vazzana, M., Schillaci, D., Russo, D., Giaramita, F.T., Parrinello, N., 2013. Gender differences in the immune system activities of the sea urchin *Paracentrotus lividus*. Comp. Biochem. Physiol. Mol. Integr. Physiol. 164, 447–455.

Arpitha, P., Prajna, N.V., Srinivasan, M., Muthukkaruppan, V., 2005. High expression of p63 combined with a large N/C ratio defines a subset of human limbal epithelial cells: implications on epithelial stem cells. Invest. Ophthalmol. Vis. Sci. 46 (10), 3631–3636.

Bainton, D.F., 1988. Phagocytic cells: developmental biology of neutrophils and eosinophils. In: Gallin, J.I., Goldsteins, I.M., Snyderman, R. (Eds.), Inflammation: Basic Principles and Clinical Correlates. Raven Press, New York NY, USA, pp. 265–280.

Baluska, F., Kubica, S., 1987. Changes in chromatin condensation during growth and differentiation of maize primary root cells. Biologia 42 (1), 9–16.

Battison, A., Cawthorn, R., Horney, B., 2003. Classification of *Homarus americanus* hemocytes and the use of differential hemocyte counts in lobsters infected with *Aerococcus viridans* var. *homari* (Gaffkemia). J. Invertebr. Pathol. 84 (3), 177–197.

Behmer, O.A., Tolosa, E.M.C., Freitas-Neto, A.G., 1976. Manual de técnicas de histologia normal e patológica. EDART/EDUSP, São Paulo.

Bertheussen, K., Seljelid, R., 1978. Echinoid phagocytes in vitro. Exp. Cell Res. 11 1, 401–412.

Bessis, G., 1977. Blood Smears Reinterpreted. Springer International, p. 270.

Bodnar, A.G., Coffman, J.A., 2016. Maintenance of somatic tissue regeneration with age in short-and long-lived species of sea urchins. Aging Cell 15 (4), 778–787.

Boudoresque, C.F., Verlaque, M., 2013. *Paracentrotus lividus* (p. 297–327). In: Lawrence, J.M. (Ed.), Sea Urchins: Biology and Ecology. Developments in Aquaculture and Fisheries Science. Elsevier Science, Amsterdam, p. 550.

Bragadeeswaran, S., Sri Kumaran, N., Prasath Sankar, P., Prabahar, R., 2013. Bioactive potential of sea urchin *Temnopleurus toreumaticus* from Devanampattinam, Southeast coast of India. J. Pharm. Altern. Med. 2 (3), 9–18.

Branco, P.C., Figueiredo, D.A.L., da Silva, J.R.M.C., 2014. New insights into innate immune system of sea urchin: coelomocytes as biosensors for environmental stress. OA Biology 18 (2), 2, 1.

Branco, P.C., Borges, J.C.S., Santos, M.F., Junior, B.E.J., da Silva, J.R.M.C., 2013. The impact of rising sea temperature on innate immune parameters in the tropical subtidal sea urchin *Lytechinus variegatus* and the intertidal sea urchin *Echinometra lucunter*. Mar. Environ. Res. 92, 95–101.

Calderón, I., Turon, X., Lessios, H.A., 2009. Characterization of the sperm molecule binding in the sea urchin genus *Paracentrotus*. J. Mol. Evol. 68, 366–376.
Calderón, I., Ventura, C.R.R., Turon, X., Lessios, H.A., 2010. Genetic divergence and assortative mating between color morphs of the sea urchin *Paracentrotus gaimardi*. Mol. Ecol. 19, 484–493.
Campbell, T.W., 2015. Exotic Animal Hematology and Cytology, fourth ed. Wiley-Blackwell, p. 424.
Caulier, G., Hamel, J.F., Mercier, A., 2020. From coelomocytes to colored aggregates: cellular components and processes involved in the immune response of the holothuroid *Cucumaria frondosa*. Biol. Bull. 239 (2), 95–114. https://doi.org/10.1086/710355.
Cervello, M., Arizza, V., Lattuca, G., Parrinello, N., Matranga, V., 1994. Detection of vitellogenin in a subpopulation of sea urchin coelomocytes. Eur. J. Cell Biol. 64 (2), 314–319.
Cheng, T.C., Guida, V.G., 1980. Hemocytes of *Bulinus truncates rohlfsi* (Mollusca: gastropoda). J. Invertebr. Pathol. 35, 158–167.
Chiaramonte, M., Arizza, V., La Rosa, S., Queiroz, V., Mauro, M., Vazzana, M., Inguglia, L., 2020. Allograft inflammatory factor AIF-1: early immune response in the mediterranean sea urchin *Paracentrotus lividus*. Zoology 142, 125815.
Chiaramonte, M., Inguglia, L., Vazzana, M., Deidun, A., Arizza, V., 2019. Stress and immune response to bacterial LPS in the sea urchin *Paracentrotus lividus* (Lamarck, 1816). Fish Shellfish Immunol. 92, 384–394.
Chiaramonte, M., Russo, R., 2015. The echinoderm innate humoral immune response. Ital. J. Zool. 82 (3), 300–308. https://doi.org/10.1080/11250003.2015.1061615.
Deveci, R., Şener, E., Izzetoğlu, S., 2015. Morphological and ultrastructural characterization of sea urchin immune cells. J. Morphol. 276 (5), 583–588.
Duarte, M., Ventura, C., Silva, E., 2016. Genetic variation in color morphs of the endangered species, *Paracentrotus gaimardi* (Echinoidea: Echinidae). Lat. Am. J. Aquat. Res. 44 (1), 46–55.
Dunham, P., Weissman, G., 1986. Aggregation of marine sponge cells induced by Ca pulses, Ca ionophores, and phorbol esters proceeds in the absence of external Ca. Biochem. Biophys. Res. Commun. 134, 1319–1326.
Dyrynda, E.A., Pipe, R.K., Ratcliffe, N.A., 1997. Sub-populations of hemocytes in the adult and developing marine mussel, *Mytilus edulis*, identified by use of monoclonal antibodies. Cell Tissue Res. 289, 527–536.
Efroni, S., Duttagupta, R., Cheng, J., Dehghani, H., Hoeppner, D.J., Dash, C., Bazett-Jones, D.P., Le Grice, S., McKay, R.D., Buetow, K.H., Gingeras, T.R., Misteli, T., Meshorer, E., 2008. Global transcription in pluripotent embryonic stem cells. Cell Stem Cell 2 (5), 437–447.
Eliseikina, M.G., Magarlamov, T.Y., 2002. Coelomocyte morphology in the holothurians *Apostichopus japonicus* (Aspidochirota: stichopodidae) and *Cucumaria japonica* (dendrochirota: cucumariidae). Russ. J. Mar. Biol. 28, 197–202.
Endean, R., 1958. The coelomocytes of *Holothuria leucospilota*. J. Cell Sci. 3 (45), 47–60. https://doi.org/10.1242/jcs.s3-99.45.47.
Faria, M.T., Silva, J.R.M.C., 2008. Innate immune response in the sea urchin Echinometra lucunter (Echinodermata). J. Invertebr. Pathol. 98 (1), 58–62.
Ferrario, C., Rusconi, F., Pulaj, A., Macchi, R., Landini, P., Paroni, M., Sugni, M., 2020. From food waste to innovative biomaterial: sea urchin-derived collagen for applications in skin regenerative medicine. Mar. Drugs 18 (8), 414.
Fontaine, A.R., Hall, B.D., 1981. The haemocyte of the holothurians *Eupentacta quinquesemita*: ultrastructure and maturation. Can. J. Zool. 59, 1884–1891.
Freshney, R., 1987. Culture of Animal Cells: a Manual of Basic Technique. Alan R. Liss (org), Inc., New York.
Gerardi, G., Lassegues, M., Canicattì, C., 1990. Cellular distribution of sea urchin antibacterial activity. Biol. Cell. 120, 161–165.
Golconda, P., Buckley, K.M., Reynolds, C.R., Romanello, J.P., Smith, L.C., 2019. The axial organ and the pharynx are sites of hematopoiesis in the sea urchin. Front. Immunol. 10, 870.
Gonzalez-Aravena, M., Perez-Troncoso, C., Urtubia, R., da Silva, J.R.M.C., Mercado, L., Lorgeril, J.D., Bethke, J., Paschke, K., 2015. Immune response of the Antarctic sea urchin *Sterechinus neumayeri*: cellular, molecular and physiological approach. Rev. Biol. Trop. 63, 309–320.
Grosch, M., Ittermann, S., Rusha, E., Greisle, T., Ori, C., Truong, D.J.J., Drukker, M., 2020. Nucleus size and DNA accessibility are linked to the regulation of paraspeckle formation in cellular differentiation. BMC Biol. 18, 1–19.
Hetzel, H.R., 1963. Studies on holothurian coelomocytes. I. A survey of coelomocyte types. Biol. Bull. 125, 289–301.
Ho, E.C.H., Rast, J.P., 2016. The immune system of echinoderms. Encyclopedia of Immunobiology 462–467. https://doi.org/10.1016/b978-0-12-374279-7.12007-7.
Holland, N.D., Phillips, J.H., Giese, A.C., 1965. An autoradiographic investigation of coelomocyte production in the purple sea urchin (*Strongylocentrous purpuratus*). Biol. Bull. 128 (2), 259–270.
Lawrence, S.M., Corriden, R., Nizet, V., 2018. The ontogeny of a neutrophil: mechanisms of granulopoiesis and homeostasis. Microbiol. Mol. Biol. Rev. 82 (1), e00057, 17.
Li, F., Zheng, Z., Li, H., Fu, R., Xu, L., Yang, F., 2021. Crayfish hemocytes develop along the granular cell lineage. Sci. Rep. 11 (1), 1–16.
Liebman, E., 1950. The leucocytes of *Arbacia punctulata*. Biol. Bull. 98, 46–59.
Lin, W., Grant, S., Beck, G., 2007. Generation of monoclonal antibodies to coelomocytes of the purple sea urchin *Arbacia punctulata*: characterization and phenotyping. Dev. Comp. Immunol. 31 (5), 465–475.
Lopes, E.M., Ventura, C.R.R., 2012. Morphology and gametic compatibility of color morphs of *Paracentrotus gaimardi* (Echinodermata: Echinoidea). Invertebr. Biol. 131 (3), 224–234.
Majeske, A.J., Oleksyk, T.K., Smith, L.C., 2013. The Sp185/333 immune response genes and proteins are expressed in cells dispersed within all major organs of the adult purple sea urchin. Innate Immun. 19 (6), 569–587.
Martoja, R., Martoja, M., 1967. Initiation aux Techniques de l'Histologie Animale. Masson et Cie, Paris, p. 354.
Matranga, V., Pinsino, A., Celi, M., Natoli, A., Bonaventura, R., Schröder, H.C., Müller, W.E., 2005. Monitoring chemical and physical stress using sea urchin immune cells. Prog. Mol. Subcell. Biol. 39, 85–110.
McCaughey, C., Bodnar, A., 2012. Investigating the sea urchin immune system: implications for disease resistance and aging. J.Young Invest. 23, 25–33.
McClay, D.R., 2011. Evolutionary crossroads in developmental biology: sea urchins. Development 138 (13), 2639–2648.
Moras, M., Lefevre, S.D., Ostuni, M.A., 2017. From Erythroblasts to mature red blood cells: organelle clearance in mammals. Front. Physiol. 8, 1076. https://doi.org/10.3389/fphys.2017.01076.
Mortensen, T.H., 1943. Monograph of the Echinoidea. III, 3. Camarodonta. II. Echinidae, Strongylocentrotidae, Parasaleniidae. Echinometridae. C.A. Reitzel, Copenhagen, p. 446.
Nieburgs, Herbert E., 1967. Nuclear/cytoplasmic ratio (N/C) and nuclear chromatin. In: Diagnostic Cell Pathology in Tissue and Smears. Grune & Stratton, New York & London, pp. 15–16.
Pagliara, P., Stabili, L., 2012. Zinc effect on the sea urchin *Paracentrotus lividus* immunological competence. Chemosphere 89 (5), 563–568.
Pantazis, P.A., 2009. The culture potential of *Paracentrotus lividus* (Lamarck 1816) in Greece: a preliminary report. Aquacult. Int. 17, 545. https://doi.org/10.1007/s10499-008-9223-5.
Pethig, R., Menachery, A., Pells, S., De Sousa, P., 2010. Dielectrophoresis: a review of applications for stem cell research. J. Biomed. Biotechnol. 2010, 182581.
Pinsino, A., Matranga, V., 2015. Sea urchin immune cells as sentinels of environmental stress. Dev. Comp. Immunol. 49 (1), 198–205.
Pinsino, A., Russo, R., Bonaventura, R., Brunelli, A., Marcomini, A., Matranga, A., 2015. Titanium dioxide nanoparticles stimulate sea urchin immune cell phagocytic activity involving TLR/p38 MAPK-mediated signaling pathway. Sci. Rep. https://doi.org/10.1038/srep14492.
Precht, L.L., Precht, W.F., 2015. The sea urchin Diadema antillarum–keystone herbivore or redundant species? PeerJ 3, e1565v1.
Queiroz, V., 2020a. An unprecedented association of an encrusting bryozoan on the test of a live sea urchin: epibiotic relationship and physiological responses. Mar. Biodivers. 50 (5), 1–7.
Queiroz, V., 2020b. Behavioral and alimentary aspects of the sea urchin *Paracentrotus gaimardi* (Echinodermata). Pesq. Ens. Ciênc. Exat. Nat. 4, e1482 https://doi.org/10.29215/pecen.v4i0.1482.
Queiroz, V., Custódio, M.R., 2015. Characterization of the spherulocyte subpopulations in *Eucidaris tribuloides* (Cidaroida: Echinoidea). Ital. J. Zool. 82 (3), 338–348.
Queiroz, V., Muxel, S.M., Inguglia, L., Chiaramonte, M., Custódio, M.R., 2021a. Comparative study of coelomocytes from *Arbacia lixula* and *Lythechinus variegatus*: cell characterization and in vivo evidence of the physiological function of vibratile cells. Fish Shellfish Immunol. 110, 1–9.
Queiroz, V., Arizza, V., Vazzana, M., Rozas, H.E., Custódio, M.R., 2021b. Cytocentrifugation as an additional method to study echinoderm coelomocytes: a comparative approach combining living cells, stained preparations, and energy-dispersive x-ray spectroscopy. Ver. Biol. Trop. 69 (S1), 171–184.
Queiroz, V., Mauro, M., Arizza, V., Custódio, M.R., Vazzana, M., 2022. The use of an integrative approach to identify coelomocytes in three species of the genus Holothuria (Echinodermata). Invertebr. Biol., e12357
Rebelo, M.D.F., Figueiredo, E.D.S., Mariante, R.M., Nóbrega, A., de Barros, C.M., Allodi, S., 2013. New insights from the oyster *Crassostrea rhizophorae* on bivalve circulating hemocytes. PLoS One 8 (2), e57384.
Romero, A., Novoa, B., Figueras, A., 2016. Cell-mediated immune response of the Mediterranean sea urchin *Paracentrotus lividus* after PAMPs stimulation. Dev. Comp. Immunol. 62, 29–38.
Sato, S., Burgess, S.B., McIlwain, D.L., 1994. Transcription and motoneuron size. J. Neurochem. 63, 1609–1615.
Schillaci, D., Cusimano, M.G., Spinello, A., Barone, G., Russo, D., Vitale, M., Parrinello, D., Arizza, V., 2014. Paracentrin 1, a synthetic antimicrobial peptide from the sea-urchin *Paracentrotus lividus*, interferes with staphylococcal and *Pseudomonas aeruginosa* biofilm formation. Amb. Express 4, 78. https://doi.org/10.1186/s13568-014-0078-z.
Schneider, C.A., Rasband, W.S., Eliceiri, K.W., 2012. NIH Image to ImageJ: 25 years of image analysis. Nat. Methods 9, 671–675.
Smith, C.L., Ghosh, J., Buckley, K.M., Clow, L.A., Dheilly, N.M., et al., 2010. Echinoderm immunity. In: Söderhäll, K. (Ed.), Invertebrate Immunity. Landes Bioscience and Springer Science BusinessMedia, New York, NY, pp. 260–301.
Smith, L.C., Arizza, V., Hudgell, M.A.B., Barone, G., Bodnar, A.G., Buckley, K.M., Sutton, E., 2018. Echinodermata: the complex immune system in echinoderms. In: Advances in Comparative Immunology. Springer, Cham, pp. 409–501.
Smith, L.C., Rast, J.P., Brockton, V., Terwilliger, D.P., Nair, S.V., Buckley, K.M., Majeske, A.J., 2006. The sea urchin immune system. Invertebr. Surviv. J. 3, 25–39.
Smith, V.J., 1981. Invertebrate blood cells. In: Ratcliffe, N.A., Rowley, A.F. (Eds.), The Echinoderms. Academic Press, New York, pp. 513–562.
Sodergren, E., et al., 2006. The genome of the sea urchin *Strongylocentrotus purpuratus*. Science 314, 941–952, 2006.
Stabili, L., Pagliara, P., Roch, P., 1996. Antibacterial activity in the coelomocytes of the sea urchin *Paracentrotus lividus*. Comp. Biochem. Physiol. B Biochem. Mol. Biol. 113 (3), 639–644.
Taguchi, M., Tsutsui, S., Nakamura, O., 2016. Differential count and time-course analysis of the cellular composition of coelomocyte aggregate of the Japanese sea cucumber *Apostichopus japonicus*. Fish Shellfish Immunol. 58, 203–590 209.

Terstappen, L.W., Safford, M., Loken, M.R., 1990. Flow cytometric analysis of human bone marrow. III. Neutrophil maturation. Leukemia 4 (9), 657–663.
Turgeon, M.L., 2012. Clinical Hematology: Theory and Procedures. Lippincott Williams & Wilkins.
Turgeon, M.L., 2005. Clinical Hematology: Theory and Procedures. Lippincott Williams & Wilkins, Hagerstwon, MD.
Vazzana, M., Celi, M., Chiaramonte, M., Inguglia, L., Russo, D., Ferrantelli, V., Arizza, V., 2018. Cytotoxic activity of *Holothuria tubulosa* (Echinodermata) coelomocytes. Fish Shellfish Immunol. 72, 334–341.
Vazzana, M., Mauro, M., Ceraulo, M., Dioguardi, M., Papale, E., Mazzola, S., Buscaino, G., 2020. Underwater high frequency noise: biological responses in sea urchin *Arbacia lixula* (Linnaeus, 1758). Comp. Biochem. Physiol. Part A Mol. Integr. Physiol. 242, 110650.
Vazzana, M., Siragusa, T., Arizza, V., Buscaino, G., Celi, M., 2015. Cellular responses and HSP70 expression during wound healing in *Holothuria tubulosa* (Gmelin, 1788). Fish Shellfish Immunol. 42 (2), 306–315.
Wołuń-Cholewa, M., Szymanowski, K., Andrusiewicz, M., Szczerba, A., Warchoł, J.B., 2010. Trichrome Mallory's stain may indicate differential rates of RNA synthesis in eutopic and ectopic endometrium. Folia Histochem. Cytobiol. 48 (1), 148–152.
Work, T.M., Millard, E., Mariani, D.B., Weatherby, T.M., Rameyer, R.A., Dagenais, J., Breeden, R., Beale, A.M., 2020. Cytology reveals diverse cell morphotypes and cellin-cell interactions in normal collector sea urchins *Tripneustes gratilla*. Dis. Aquat. Org. 19 (142), 63–73.
Xing, K., Yang, H.S., Chen, M.Y., 2008. Morphological and ultrastructural characterization of the coelomocytes in *Apostichopus japonicus*. Aquatic Biol. 2, 85–92. https://doi.org/10.3354/ab00038.